Sensors and Actuators B 240 (2017) 543–552

Contents lists available at ScienceDirect

Sensors and Actuators B: Chemical

journal homepage: www.elsevier.com/locate/snb

Emergence of the selective ultra-sensing of Ag(I): Thiolactic acid as efficient capping agent for cadmium chalcogenide quantum dots in modulating photoluminescence and metal reception

Niharendu Mahapatra [a], Abhijit Mandal [b], Sudipta Panja [a], Mintu Halder [a,*]

[a] Department of Chemistry, Indian Institute of Technology Kharagpur, Kharagpur 721302, India
[b] Department of Chemistry and Environment, Heritage Institute of Technology, Kolkata 700107, India

ARTICLE INFO

Article history:
Received 8 April 2016
Received in revised form 20 August 2016
Accepted 22 August 2016
Available online 30 August 2016

Keywords:
Selective-ultrasensitive detection
Ag(I) sensing
Turn-off-photoluminescence
Capping ligand
TLA-CdTe quantum dots

ABSTRACT

Stable and water-soluble cadmium telluride quantum dots (CdTe QDs) have been employed for ultra-sensing exclusive to water soluble Ag(I). For this purpose we have designed and synthesized thiolactic acid (TLA) capped exquisite CdTe QDs having exclusive selectivity for silver. The limit of detection (LOD) of Ag(I) is 50 nM. The pendant methyl group of TLA effectively impedes the precursor aggregation by inhibiting the secondary coordination of carboxyl oxygen of mercapto acid with the surrounding Cd(II), and this results in highly luminescent TLA-CdTe QDs. This pendant methyl group of TLA also facilitates exclusive surface adsorption of QDs by incoming metal and renders sensing selectivity. Selective adsorption of silver on TLA-CdTe QD surface provides a turn-off photoluminescence-based assay for sensitive detection of Ag(I) without any interference of other commonly coexisting metal ions. Furthermore, analyses of environmental water samples spiked with Ag(I), demonstrate immense practical potential of our TLA-CdTe QD sensor for the detection of silver in real samples. The results also unveiled the possible origin of the sensing selectivity for metal ion by TLA-capped QDs which can serve in the design and selection of appropriate capping in achieving the desired sensing selectivity.

1. Introduction

Semiconductor nanocrystals, known as quantum dots (QDs), are of great interest due to their unique optical properties [1–3] which make their fascinating applications in the areas from optics, bioimaging, labeling, sensing, gene-drug delivery and so on [2,4–18]. Till date, two methods have been employed to synthesize water soluble QDs: (1) high temperature decomposition of hazardous organometallic precursors in organic solvents followed by a post-treatment based on either ligand exchange or hydrophilic shell growth on the pre-synthesized hydrophobic QDs to transfer into water, and (2) direct aqueous synthesis with water soluble capping ligands [19–23]. The former one is somewhat technically complicated, suffers from aggregation and photoluminescence (PL) quenching during the post-treatment steps [24,25]. Consequently, increasing efforts have been made to improve simple, facile, and low-cost direct aqueous synthesis methods for water-soluble QDs with adequate hydrophilic surface capping agents to promote effectively the biological and sensing applications of QDs in aqueous solution.

Among various hydrophilic capping ligands, use of mercapto acids is a key point to obtain highly luminescent QDs [26]. To date, several types of mercapto acids have been used as capping agents and most of them contain a single mercapto function and a single carboxyl group, such as thioglycolic acid (TGA) and 3-mercaptopropionic acid (MPA) etc [27]. These mercapto acids have considerable differences, especially in terms of the nature of surface passivation, which in turn affects the growth rate, stability and PL properties of the QDs. Current research activities in literature reveal that both the two factors like chain length for the hydrophilicity-liophobicity balance (HLB) and also secondary coordination of mercapto acids play important roles during aqueous synthesis in order to control the growth and PL of QDs [28]. Both TGA and MPA have a terminal carboxylic acid group, which can form the secondary coordination between carboxyl oxygen and cadmium [28,29]. The longer chain of MPA facilitates the coordination of the thiol sulfur (primary coordination) and the carboxyl oxygen (secondary coordination) with the same cadmium site, leading to the most favorable hexagonal configuration. As TGA is shorter

* Corresponding author.
E-mail addresses: mintu@chem.iitkgp.ernet.in, mhchem@gmail.com (M. Halder).

http://dx.doi.org/10.1016/j.snb.2016.08.127
0925-4005/

than MPA by one methylene unit, the carboxyl oxygen of TGA may coordinate with the cadmium site adjacent to that initially capped by the thiol sulfur to cause aggregation of the precursors [28,29], which is unfavorable in achieving highly luminescent QDs.

Herein, thiolactic acid (TLA) has been used as capping ligand having the same main chain length as TGA with a pendant methyl group in the side chain which can inhibit the secondary coordination of carboxyl oxygen with the surrounding cadmium and stop the aggregation process [28]. Moreover, existing literature report reveals that luminescence intensity of CdS QDs capped with TLA is better than that with MPA [30]. Hence, in an effort to produce stable and highly luminescent QDs, TLA has been chosen as the capping ligand for hydrothermal synthesis of the CdTe QDs. A detailed study has been performed on the influence of process variables such as pH, reflux time, Cd/Te molar ratio, and TLA/Cd molar ratio on particle properties, such as size and PL behavior.

Recent advances in nanocrystalline materials have generated incredible interest on their applications in the detection of several ions and biomolecules etc. by making use of their superior luminescence properties and stability in aqueous solutions [2,31–35]. Till date, mercapto acid-capped QDs pose great promises towards selective detection of several ions [31,35,36]. However, the reason behind the selectivity is not very clear, and the potential function of the mercapto acid structure toward sensing selectivity is still a relevant question. Herein, an exploration of the importance of the structural effect of TLA-capping ligand towards metal ion sensing selectivity of QDs has been attempted.

Selective detection of Ag(I) is important due to its toxicity related problems, although it has been extensively used as silver nanoparticle (Ag NPs) in various commercial products owing to their antimicrobial and catalytic properties [37]. Naturally occurring silver in soils, water or in commercial products may be absorbed in human and animals, by the gastrointestinal tract, skin, mucous and membranes, which can cause argyria and/or argyrosis [38]. Ag(I) ions are highly toxic to aquatic organisms and may accumulate in the human body through the food chain [39]. When absorbed in the human body, silver ions can displace essential metal ions such as Ca(II) and Zn(II) ions in hydroxyl apatite in bone. The high concentration of Ag(I) ion can lead to bioaccumulation and variety of adverse health effects, inactivation of sulfhydryl enzymes, brain damage, nerve damage and immune systems. Therefore, the analysis of Ag(I) ions in water and food resources is of great importance. The free silver ion, Ag(I), is known to be more toxic to aquatic organisms than other silver species [40–42]. Therefore, the need for a highly sensitive and selective determination of silver ion arises from its long-term toxicity for human and the environment.

On the application side, here we have demonstrated a turn-off PL-based assay for sensitive and selective detection of Ag(I) in aqueous solution using TLA-capped CdTe QDs (TLA-CdTe QDs) in presence of other commonly coexisting metals, e.g., Zn(II), Cr(II), Al(III), Cd(II), Co(II), Ni(II), Pb(II), Ca(II), Na(I), K(I), Hg(II), Fe(II), Fe(III), La(III), Au(III), Cu(II). Although, several reports for Ag(I) detection using QDs have been documented [32,43,44], but most of them suffer from either tedious preparation of the sensor, and/or limit of detection (LOD), and/or interference of other coexisting metal ions. For example, Zhang et al. reported that surface modified (with iminodiacetic acid) Mn(II) doped ZnS QDs can act as luminescent probe for Ag(I) in phosphate buffer solution (pH 7.3) with a detection limit of 2.6×10^{-7} mol/L using PL quenching technique [43]. Mandal et al. reported a simple TLA capped ZnS QDs based PL quenching technique for sensing of Ag(I) within the range of $5 \times 10^{-7} - 1 \times 10^{-6}$ mol/L [32]. Gan et al. reported a simple MPA-capped CdTe QDs based PL turn-off assay for detection of Ag(I) with a good detection limit of 4.106×10^{-8} mol/L, but it suffers from the interference of Cu(II) [44]. Hence, the development of highly sensitive and selective strategy for the detection of Ag(I) in trace in their sources is of great importance to minimize the anticipated toxic effects. Interestingly, our TLA-capped CdTe QD sensor is easy to prepare, has high LOD and also doesn't suffer from the interference of other commonly coexisting metals than the literature reported QDs-based sensors [32,43,44]. In order to demonstrate the practical applicability of the PL-based sensing assay, the detection of Ag(I) has also been performed in real water samples. Herein, we have also discussed the mechanism of PL quenching of QDs by Ag(I). The potential role of pendent methyl group of TLA capping ligand towards metal ion sensing selectivity has also been demonstrated.

2. Experimental

2.1. Materials

All analytical grade reagents are used for this study. Cadmium chloride ($CdCl_2$), thiolactic acid (TLA) and tellurium (Te) powder (99.997% trace metals basis) are purchased from Sigma Aldrich. Sodium borohydride ($NaBH_4$), sodium hydroxide (NaOH) and all the soluble metal salts used for sensing experiments are purchased from Merck. For all experiments the aqueous solutions are prepared only with deionized water.

2.2. Instrumentation

Eutech-510 ion pH-meter, pre-calibrated with standard pH buffer tablets, is used for pH measurement. UV-2450 (Shimadzu) absorbance spectrophotometer is used to record the electronic absorption spectra against solvent reference. Hitachi-7000 spectrofluorimeter is employed to record the steady state PL spectra. The PL lifetime decay is recorded with a single photon counting apparatus (Horiba, Jobin Yvon, IBH Ltd., Glasgow, Scotland) with an excitation source of 377 nm. All the decays are collected at the corresponding emission maxima at magic angle 54.7° employing a Hamamatsu microchannel plate (MCP) photomultiplier tube (R3809U). Analysis of the decays are done, as sum of the exponential components with pre-exponential factors (α_i) normalized to unity, applying iterative reconvolution with IBH DAS-6 software. The χ^2 values and weighted residuals ensure the perfectness of fit. JEOL Model JEM-2010 electron microscope with an operating voltage of 200 kV is used for taking transmission electron microscopy (TEM) images. Composition analysis is performed by using energy-dispersive X-ray spectroscopy (EDX) measurements. Bruker D8 diffractometer unit with nickel-filtered Cu Kα line (λ = 1.54 Å) is used for collecting the X-ray diffraction (XRD) pattern of the sample within the 2θ range of 15°–90° at a scanning rate of 3.0° min^{-1}. JCPDS software is used for the XRD data analysis. X-ray photoelectron spectroscopic (XPS) studies are carried out with PHI 5000 *VersaProbe* II scanning XPS microprobe (ULVAC-PHI, inc.) using the energy source Al (Kα, $h\nu$ = 1486.6 eV).

2.3. Preparation of sodium hydrogen telluride

NaHTe is prepared according to the method described elsewhere [45] with some modifications as follows. The molar ratio of tellurium (Te) powder and sodium borohydride is 1: 3. Briefly, 16 mg of Te powder is taken in a small round bottom flask and to it 4 ml water is added. After that, 14 mg of sodium borohydride is added in the flask, the reacting system is cooled on ice bath (~3°C). After approximately 4 h, the black Te powder disappears and a white precipitate of sodium tetraborate appears at the bottom of the flask. The resulting clear supernatant of NaHTe is used for the preparation of CdTe particles.

2.4. Synthesis of water-soluble TLA-CdTe QDs

Required amount of $CdCl_2$ and TLA are dissolved in water, so that the concentration ratio becomes 1: 2.4, where [$CdCl_2$] = 2.35 mM [45]. The desired pH is attained by the drop-wise addition of 1 M NaOH solution to the above mixture. The solution is deaerated with N_2 bubbling for 30 min. Then required volume of freshly prepared NaHTe solution is injected to the above mixture under stirring and N_2 bubbling condition. The molar ration of Cd: Te: TLA was fixed to 1: 0.5: 2.4. The N_2 bubbling and stirring are continued for another 30 min after complete addition of NaHTe solution.

The size of the TLA-CdTe QDs is controlled by the duration of reflux time and monitored by absorption and emission measurements. TLA-CdTe QDs syntheses have been performed for different pH (7–12) of the initial reaction mixture at a fixed molar ratio of the precursors (Cd: Te: TLA = 1: 0.5: 2.4). The variation of molar ratio of the precursors is performed at pH 9 only, as at this pH the PL intensity of the synthesized TLA-CdTe QDs is found to be maximum. Three different Cd/Te molar ratios and five different TLA/Cd molar ratios are attempted to optimize the PL intensity of TLA-CdTe QDs. The ratio of [Cd]: [Te]: [TLA] = 1: 0.5: 2.4 was found to be optimal to obtain the highest PL intensity. Conventional studies, such as UV–vis and PL spectroscopy, PL lifetime measurements, TEM and XRD are performed to characterize the synthesized TLA-CdTe QDs.

2.5. Sensitive and selective detection of Ag(I) with TLA-CdTe QDs

Turn-off PL-based protocol for selective detection of Ag(I) at room temperature is performed by using our synthesized TLA-CdTe QDs at pH 9.0 obtained after 4 h reflux having maximum PL intensity. Deionized water is used to prepare the desired concentration of all metal ions from their respective salts and stored at room temperature (~25 °C). The final concentration of the metal is achieved by mixing the required volume of a particular metal ion solution with TLA-CdTe QDs solution and used to monitor the change in absorbance, PL intensity, PL lifetime decay, and XPS of QDs.

2.6. Analysis of real samples

To evaluate the application potential of the sensing assay in real sample analysis, the sensor has been applied to analyze pond water and tap water samples, collected from IIT Kharagpur campus. The collected pond water and tap water samples are boiled and cooled to room temperature, and then filtered with the qualitative filter paper. These water samples are spiked with solution of Ag(I), and then an appropriate volume of the spiked sample is added to TLA-CdTe QD solution in order to achieve the desired Ag(I) concentrations, and finally all the measurements are performed by following the same procedures as discussed above.

3. Results and discussion

3.1. Tunable optical properties of TLA-CdTe QDs

The steady state absorption and photoluminescence (PL) spectra of size selected fractions of TLA-CdTe QDs for different pH at a fixed molar ratio of the precursors (Cd: Te: TLA = 1: 0.5: 2.4) are shown in Supplementary information S1 (Fig. S1A–F). For all starting pH, large red shifting of the absorbance peak position and increase in absorbance reveal that both the particle size and number density of particles increase during refluxation. The large Stokes-shifted emission maxima (approximately about 1 eV lower than the absorption edge) indicate the involvement of trap-states (lattice defects) in PL of the QDs. Relatively stronger luminescence intensity and maximum stability of the QDs appear at pH 9, which may be due to better crystallization and surface capping. During refluxation, pH can influence on the nucleation and growth rate, and after synthesis, pH can also affect on the stability and aggregation behavior of the colloids. Before the addition of telluride, Cd(II) forms complexes with TLA and the type and stability of these complexes are pH dependent, which can influence on the particle properties [30]. Below pH 5, insoluble complexes are formed, which dissolve with increase of pH, possibly due to better complexation between Cd(II) and TLA. Thus, one can expect a well controlled growth of the particles, which allows better crystallinity and surface passivation at pH 9 [30]. Above pH 9, the increase in charge density on the particle surface may hinder the attachment of TLA molecules (anion) onto the surface, leading to increase in the number of uncoordinated sites, which may result in the decrease of PL intensity and stability also [30]. Again at high pH decrease in solubility of CdTe may also affect the photoluminescence intensity as well as stability.

Generally, Cd/Te ratio is effective in determining the size of the QDs. Variation of Cd/Te molar ratio (from 4 to 1) is performed at pH 9 by keeping the TLA/Te molar ratio (at 4.8) fixed. Corresponding UV–vis and PL spectra with respect to reflux time are shown in Supplementary information S2 (Fig. S2A–C). Here also, for all different Cd/Te ratios the absorption peak position gets red shifted (i.e., particle size increases) during refluxation. But the noticeable feature is that with the decrease in Cd/Te ratio from 4 to 2, a huge blue shift in absorbance edge occurs, which indicates a large decrease in particle size. In PL spectra also, very little Stokes shift reveals that band-edge emission occurs at Cd/Te ratio of 4, which is converted to large Stokes shifted trap-state emission at Cd/Te ratio of 2. Different types of nucleation process could be the possible origin of the above facts. These affect the quality of the nanocrystal structures resulting in different types of luminescence pattern. Further decrease in Cd/Te ratio (from 2 to 1) has almost negligible effect on the absorbance property but results in the decrease of luminescence intensity. Thus, the experimental results indicate that the best batch TLA-CdTe QDs with strong luminescence intensity can be synthesized at the Cd/Te ratio of 2.

In order to check the effect of capping agent on the optical properties of TLA-CdTe QDs, we have performed the variation of TLA/Cd molar ratio at a fixed Cd/Te ratio of 2 at pH 9. The UV–vis and PL spectra for different TLA/Cd ratios are shown in Supplementary information S3 (Fig. S3A–E). For any TLA/Cd ratio the absorption peak position is found to be red shifted (i.e., particle size increases) with increase of refluxing time. But for different TLA/Cd molar ratios, within the range from 1 to 4.8, there is no dramatic change in absorbance spectra, and all the QDs yield a large Stokes shifted emission profile. The only difference is in luminescence intensity which is found to be maximum at a TLA/Cd molar ratio of 2.4. The possible reason for this is that at low concentration of capping agent enough surface coverage is not achieved to arrest the surface defects, resulting in nonradiative recombination. At relatively lower concentration of TLA there is a fair chance to form clusters of CdTe QDs, and as a result, poor dispersion of TLA-CdTe QDs occurred. Due to this, the emission intensity was suppressed noticeably. After sufficient amount of coating, addition of excess TLA leads to the surface crowding, which may result in the decrease of PL intensity. This reveals that TLA/Cd ratio has considerable effect on particle surface construction rather than crystal growth. So, highly luminescent TLA-capped CdTe QDs with substantial surface passivation can be synthesized at a TLA/Cd molar ratio of 2.4.

It is evident from Fig. 1 that in optimized synthesis conditions red shifted absorption spectra of TLA-CdTe QDs ([$CdCl_2$]: [Te]: [TLA] = 1: 0.5: 2.4 at pH 9, where [$CdCl_2$] = 2.35 mM) indicate rapid growth and increase in size of the QDs with increase in refluxing time upto 4 h. This is also confirmed from TEM measurements (Fig. 2A and B). On the other hand, the large Stokes-shifted trap-states PL of TLA-CdTe QDs originates from lattice defects within the nanocrystals. The Cd and Te, vacancies and interstitials are

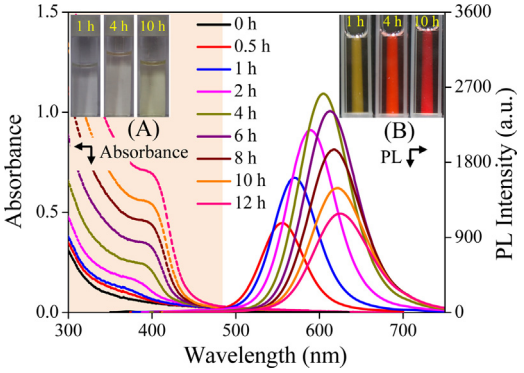

Fig. 1. Reflux time dependent (A) Absorbance (dotted line) and (B) photoluminescence (solid line) spectra of TLA-CdTe QDs synthesized in aqueous solution and at a fixed [Cd]: [Te]: [TLA] molar ratio of 1: 0.5: 2.4 and pH 9, where $[CdCl_2] = 2.35$ mM. Insets are the photographs of the QD solutions in daylight (left side) and UV light (right side) at different reflux time.

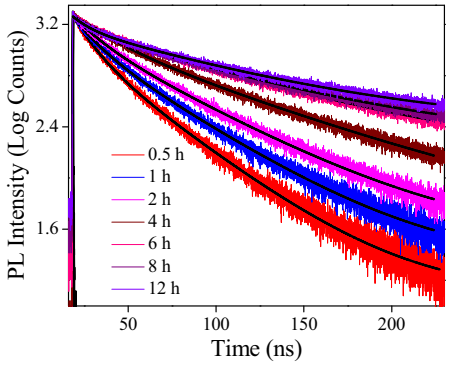

Fig. 3. Room temperature PL decay curves of TLA-CdTe QDs in aqueous solution obtained at different reflux time. TLA-CdTe QDs are synthesized at a fixed [Cd]: [Te]: [TLA] molar ratio of 1: 0.5: 2.4 and pH 9, where $[CdCl_2] = 2.35$ mM. All the samples are exited with a 377 nm pulsed laser source and the decays are collected at their corresponding PL peak.

the main atomic defects in the CdTe nanocrystals. The PL intensity increases upto 4 h of reflux time and beyond 4 h refluxation, luminescence intensity decreases despite the increase in absorbance. The decrease in PL intensity may be due to either clustering as evident from TEM image (Fig. 2C) or decrease in population of the defect states with increase in reflux time [2]. In clusters, various size distribution and close proximity between the particles facilitate the transfer of the excitation energy of one QD to another in a non-radiative way, which could suppress the PL.

Since quantum confinement is lost due to clustering, the densely packed state within the cluster would render the particle to behave like bulk CdTe, which may result in the substantial decrease in luminescence intensity during further refluxation [2]. As a result, these QDs show size and proximity dependent trap-state PL as discussed by us elsewhere [2]. Thus in our case, with increase in refluxation time, i.e., with the increase of nanocrystal size and degree of clustering, the trap-state PL peaks of the said QDs get largely red shifted (556 nm → 625 nm) [46,47].

Fig. 3 represents the initial part of PL lifetime decay profiles of TLA-CdTe QDs synthesized by utilizing the optimized condition at different reflux time. Our synthesized TLA-CdTe QDs show multi-exponential PL decay behaviors [31,36,48]. Interaction of various types of defect states with their environments may result in such complex PL decays. The decay curves show a reasonably good biexponential fitting and the estimated approximate lifetime parameters are highlighted in Table 1. Previous literature reports reveal that the faster lifetime component is associated with the

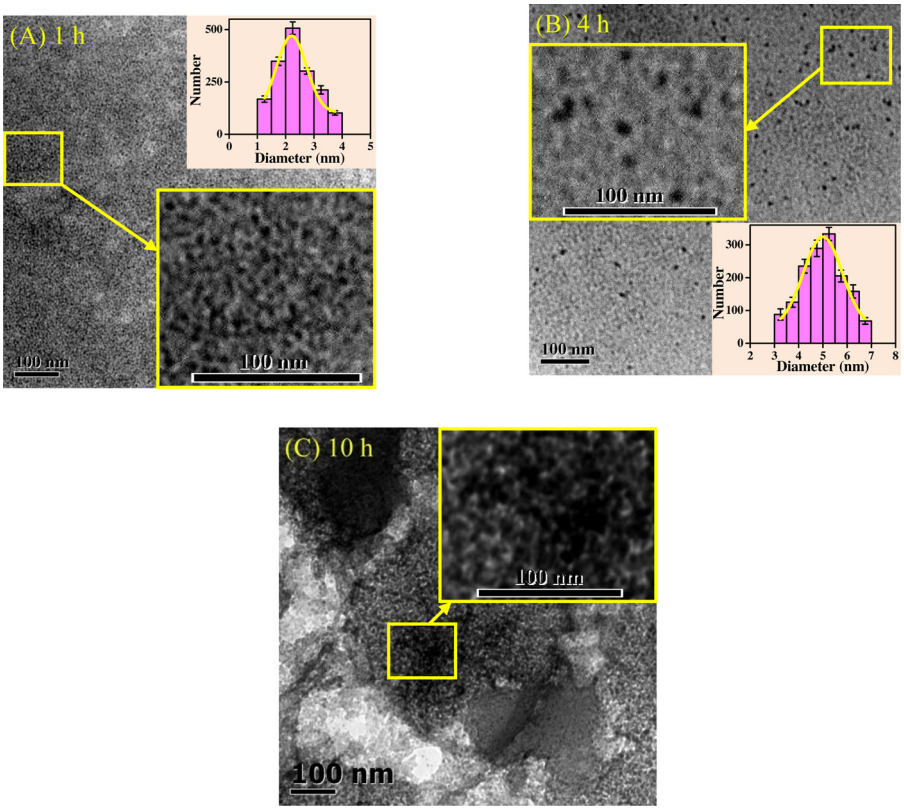

Fig. 2. Reflux time dependent, (A) 1 h, (B) 4 h and (C) 10 h, TEM images of TLA-CdTe QDs synthesized in aqueous solution and at a fixed [Cd]: [Te]: [TLA] molar ratio of 1: 0.5: 2.4 and pH 9. The insets show the particle size distribution at corresponding condition.

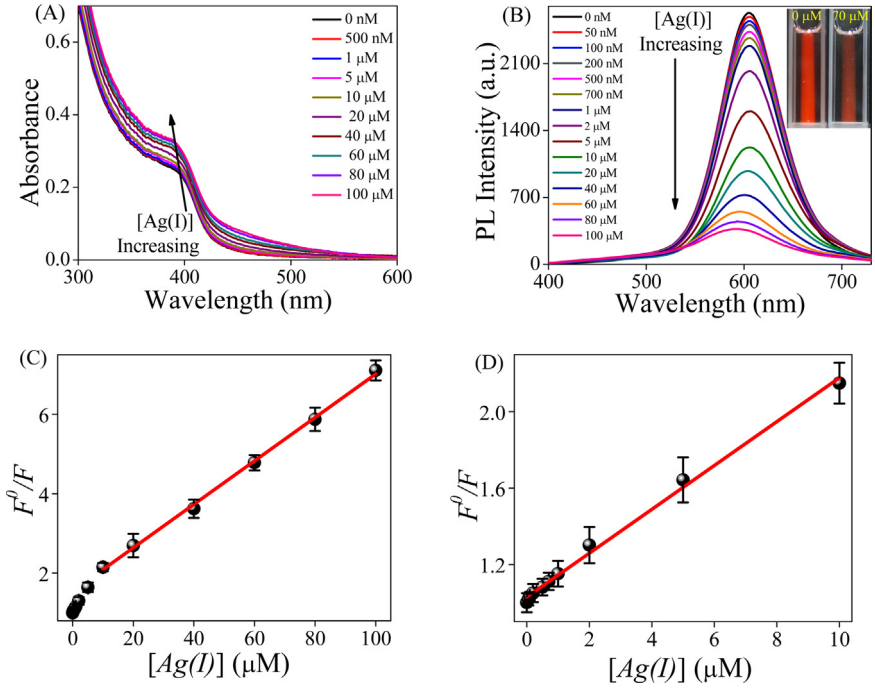

Fig. 4. Ag(I) concentration dependent (A) UV–vis and (B) PL spectra of TLA-CdTe QDs synthesized at a fixed [Cd]: [Te]: [TLA] molar ratio of 1: 0.5: 2.4 and pH 9, where [$CdCl_2$] = 2.35 mM, after 4 h refluxation. Inset of B is the photographs of QD solutions in the absence and presence of Ag(I), under UV light. Plots of relative PL intensity (F^0/F) *vs* [*Ag(I)*], for (C) whole range of concentration and (D) lower range of concentration.

intrinsic recombination of populated core-states, while the longer lifetime component is due to the surface-related radiative recombination of carriers [32,36]. The substantially high weight of the surface-related longer lifetime component (α_2) is usually well correlated with higher luminescence intensity [36,49]. The different lifetime component arises from the variation of the nonradiative decay rates caused by the trap states [32,50]. The increase in longer lifetime component indicates the involvement of more surface states in the PL process. Beyond 6 h refluxation, in spite of the substantial decrease in steady state PL intensity, the lifetime has been found to remain almost constant, which indicates that the amount of defect state doesn't change thereafter.

3.2. Characterization studies of TLA-CdTe QDs

Fig. 2 represents the TEM images of TLA-CdTe QDs synthesized by our optimized condition after 1 h (Fig. 2A), 4 h (Fig. 2B) and 10 h (Fig. 2C) refluxation. The TLA-CdTe QDs show mostly spherical shapes with diameter in the range between 1 nm to 3.5 nm and 3 nm to 7 nm after 1 h and 4 h refluxation, respectively, as evident from the statistical size distribution histograms (Fig. 2A and B, inset). At a considerably longer reflux time clustering occurs (as evident from Fig. 2C), which may cause the decrease in luminescence intensity. The complete characterization of our synthesized TLA-CdTe QD has been provided in the Supplementary information S4.

Table 1
Refluxing time-dependent estimated values of lifetimes (τ), relative amplitudes (α), average lifetimes (τ_{av}) and χ^2, obtained from the fitted initial part of PL decay of water soluble TLA-CdTe QDs synthesized at a fixed [Cd]: [Te]: [TLA] molar ratio of 1: 0.5: 2.4 and pH 9, where [$CdCl_2$] = 2.35 mM[a].

Reflux time (*h*)	α_1	τ_1 (ns)	α_2	τ_2 (ns)	τ_{av} (ns)	χ^2
0.5	0.1796	11.55	0.8204	41.61	36.21	1.133
1	0.1323	13.37	0.8677	49.12	44.39	1.074
2	0.1030	14.73	0.8970	57.77	53.34	1.049
4	0.1240	23.23	0.8760	87.16	79.23	1.056
6	0.0526	17.16	0.9474	96.49	92.32	1.052
8	0.0415	12.62	0.9585	92.75	89.42	1.040
12	0.0308	10.14	0.9692	93.97	91.39	1.049

[a] Errors in estimation of lifetimes: ~±5%.

3.3. Sensitive and selective turn-Off-PL of TLA-CdTe QDs by Ag(I)

We have observed that Ag(I) quenched the PL of our synthesized TLA-capped CdTe QDs in a concentration dependent manner. Therefore, in order to study the effect of Ag(I) concentration on the PL, we used TLA-CdTe QDs with maximum luminescence intensity i.e., TLA-CdTe QDs obtained by our optimized conditions after 4 h reflux time. Fig. 4B represents the decrease in PL intensity of TLA-CdTe QDs with increasing concentration of Ag(I). Almost full quenching of the PL intensity of QDs occurs within the concentration range of 50 nM to 100 μM. Therefore, the synthesized TLA-CdTe QDs can be used to develop a sensitive turn-off PL based assay for the detection of Ag(I). To explore the sensitivity of the PL-quenching technique, we have plotted the relative luminescence intensity (F^0/F) with respect to Ag(I) concentration (Fig. 4C and D), where F^0 and F are the PL intensities of TLA-CdTe QDs at 605 nm in the absence and presence of Ag(I), respectively. The plot of F^0/F *vs* [*Ag(I)*], over the whole concentration range can be fitted in two linear segments: (1) from 50 nM to 10 μM (Fig. 4D), and (2) from 10 μM to 100 μM (Fig. 4C). For the two different concentration ranges, the linear equations with linearity coefficients are shown in Table 2, from which one can estimate the unknown concentration of Ag(I). Evaluation of limit of detection (LOD) can be carried out by using the equation LOD = (3σ/k), where σ stands for

Table 2
Linear equations and linearity coefficients of F^0/F *vs* [*Ag(I)*] plot at different concentration ranges.

Concentration range of Ag(I)	Linear equation	Linearity coefficient
50 nM–10 μM	$F^0/F = 0.115[Ag(I)] + 1.029$	0.995
10 μM–100 μM	$F^0/F = 0.055[Ag(I)] + 1.547$	0.998

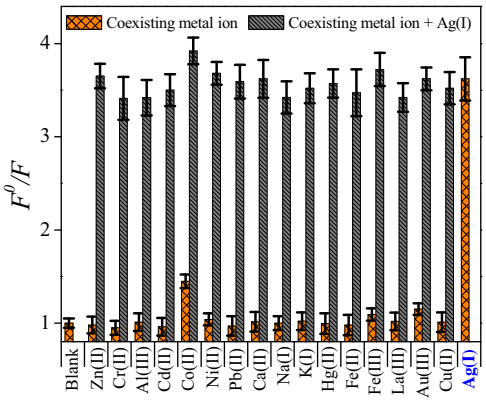

Fig. 5. Plot of relative PL intensity (F^0/F) of TLA-CdTe QDs for a fixed concentration (40 μM) of different metal ions. Orange bars represent the responses from individual metals and the gray bars indicate the responses from Ag(I) in the presence of other coexisting metals. (For interpretation of the references to colour in this figure legend, the reader is referred to the web version of this article.)

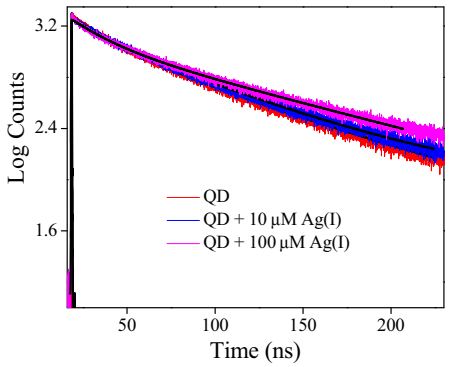

Fig. 6. PL lifetime decay profiles of TLA-CdTe QDs in the absence and presence of different concentrations of Ag(I). The samples are exited with a 377 nm pulsed laser source and all the decays are collected at their emission maxima and at room temperature.

the standard deviation of the y-intercepts of regression lines, and k represents the slope of calibration graph [2,51]. The LOD of Ag(I) is ~50 nM, which is far better in comparison with other literature reports [32,43].

To determine the selectivity of Ag(I) detection by the TLA-CdTe QD senor, we have performed the PL quenching with different physiologically important metal ions and also with some transition metal ions (as stated earlier in the introduction section). Experimental results reveal that other common metal ions have almost no influence on the photoluminescence intensity of the TLA-CdTe QDs. We have plotted F^0/F for the TLA-CdTe QD in the presence of some fixed concentration (40 μM) of different metal ions (bar plot of Fig. 5), where F^0 and F are the PL intensities in the absence and presence of metals, respectively. Except for Ag(I), almost unity values of F^0/F for all other common metals indicate their inability to quench the PL of TLA-CdTe QDs. This shows exclusive selectivity of Ag(I) in quenching of PL of the synthesized QDs. Moreover, competitive studies, i.e., PL quenching of TLA-CdTe QDs by Ag(I) in the presence of other metal ions, are also performed. As shown in Fig. 5, substantial change in relative PL intensity (F^0/F) occurs due to the addition of Ag(I), either in the absence in presence of other metals. The selective detection of Ag(I) through PL quenching, is hardly affected in presence of these commonly coexisting ions. This reveals that the TLA–CdTe QDs exhibited excellent selectivity for Ag(I) in the presence of other metal ions. Hence our synthesized TLA-CdTe QDs can be used as a turn-off PL-based sensor for sensitive and selective detection of Ag(I).

3.4. Detection of Ag(I) in real samples

These initial results endorse the efficiency of our proposed sensing assay to detect Ag(I) in the presence of different co-existing metals. But the detection of Ag(I) in real samples is much more challenging goal, since most of the sensors are not stable enough in a complicated environment. To evaluate the practicality of our proposed sensing assay, we have employed our TLA-CdTe QD sensor for the analysis of real environmental samples (pond water and tap water) spiked with different Ag(I) concentrations. The maximum spiked Ag(I) concentration is upto 200 nM, as the chloride content of our collected real environmental samples are ~700 μM and the solubility product (K_{sp}) of AgCl is 1.8×10^{-10} at 25° C [52,53]. The treated real water samples spiked with different concentrations of Ag(I) (0, 50, 100 and 200 nM), are tested employing the same procedure as discussed above. The results obtained, are summarized in the Supplementary information S5 and indicate good recovery, which validates that our proposed PL-based TLA-CdTe QD sensor can also be useful for real environmental water samples analysis.

3.5. Mechanism of Ag(I) detection by TLA-CdTe QDs

PL quenching of QDs by metals is a complex process and several mechanisms such as energy transfer, electron transfer, non-radiative recombination pathways, ion-binding etc. have been proposed [2,31,32,36,44]. Earlier literature reports reveal that Ag(I) affects the PL of QDs through adsorption onto the particle surface [31,32,36,44]. The adsorbed metal can control the PL behavior of QDs either by simple interaction with surface trap-states or by the effective removal of surface trap-states through the formation of metal chalcogenides (e.g. AgTe) with dangling bonds of chalcogens [32,36,44]. The simple interaction of metal with surface trap-states can lead to increase or decrease of PL of QDs with a very little shift of the absorption and PL peak position. On the other hand, the effective removal of surface trap-states should be associated with large shifts of both absorption and PL peak position with a noticeable change in spectral profile [36]. In the present case, we have found a very little shift of absorption peak position (Fig. 4A) and a little blue-shift (~12 nm) of PL peak position (Fig. 4B) of TLA-CdTe QDs. This indicates that simple interaction of surface adsorbed Ag(I) with trap-states of QDs results in the PL quenching either by energy transfer or by electron transfer or by non-radiative recombination processes. Practically unchanged PL lifetime of TLA-CdTe QDs before and after addition of Ag(I) (Fig. 6) further indicates that AgTe formation does not take place through the elimination of dangling bonds of Te on the particle surface [31,36,54–56]. No change in PL lifetime also negates the possibility of PL quenching either by energy transfer or by electron transfer process [31,36,57–59]. So, we can presume that the adsorption of Ag(I) onto the surface of TLA-CdTe QDs can reduce the recombination luminescence by stimulating the non-radiative electron/hole recombination process at the previously existing defect sites on the nanocrystals surface [60,61].

XPS studies are carried out to confirm the binding of silver ion onto the nanocrystal surface, since XPS provides information about the surface chemical composition and the chemical states of nanomaterials [62]. Here, Cd 3d, Te 3d and Ag 3d core levels have been focused. The spectra of the Cd 3d, Te 3d and Ag 3d core levels are represented in Fig. 7A, B and C, respectively. The appearance of Cd $3d_{5/2}$ peak at 405.1 eV, Cd $3d_{3/2}$ peak at 411.9 eV, Te $3d_{5/2}$ peak at 572.4 eV and Te $3d_{3/2}$ peak at 582.7 eV ensure the presence of cadmium and tellurium in the TLA-CdTe QDs, which is in good agreement with the existing literature reports [12,63]. After addition of silver ions (50 μM) to TLA-CdTe QDs, the appearance of Ag

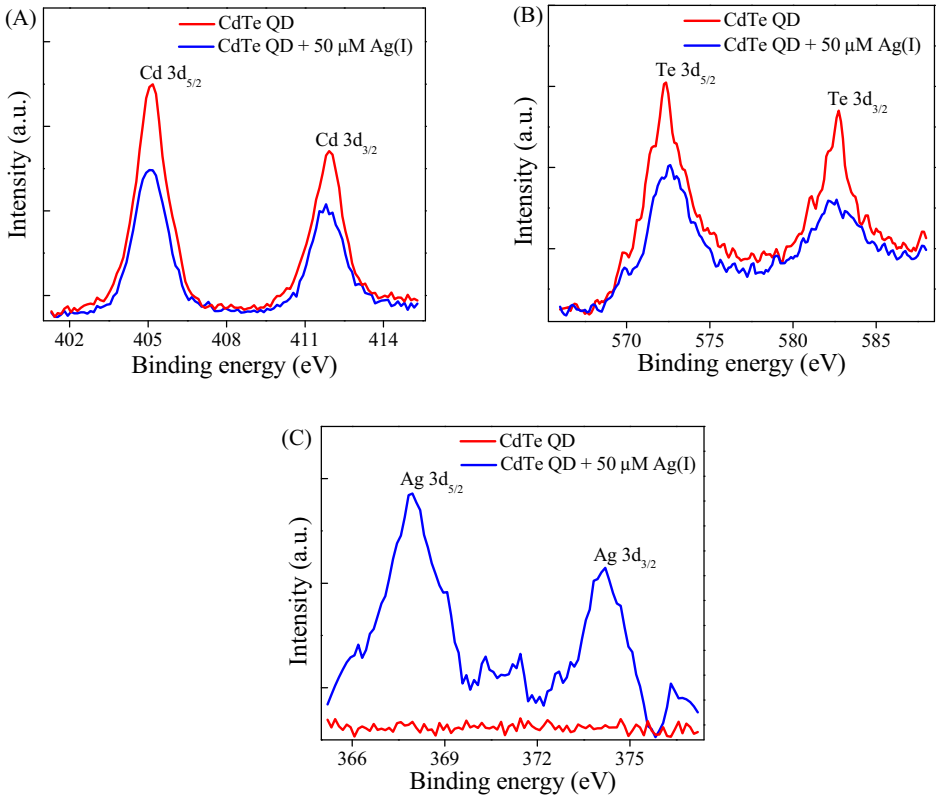

Fig. 7. (A) Cd 3d, (B) Te 3d and (C) Ag 3d core levels XPS spectra of TLA-CdTe QDs in the absence and presence of 50 μM Ag(I).

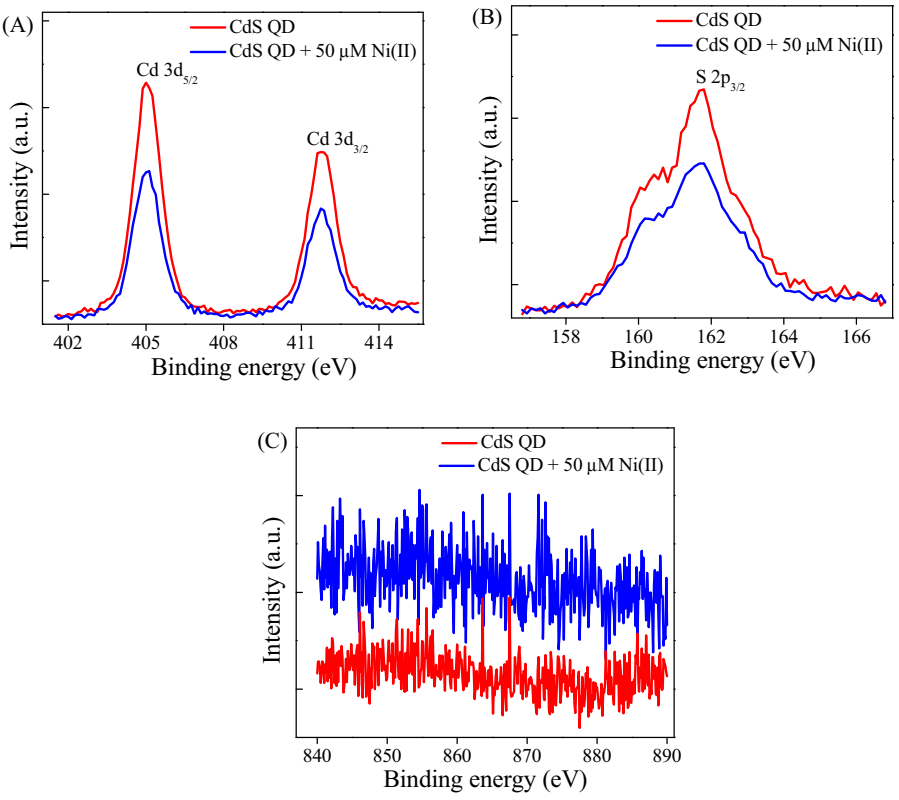

Fig. 8. (A) Cd 3d, (B) S 2p and (C) Ni 2p core levels XPS spectra of MPA-capped CdS QDs in the absence and presence of 50 μM Ni(II).

$3d_{5/2}$ peak at 367.9 eV and Ag $3d_{3/2}$ peak at 374.1 eV [62,64] confirm the binding of Ag onto the nanocrystal surface.

In order to reinforce the phenomenon of binding of Ag onto the nanocrystal surface, further XPS studies are also carried out for Ni(II) induced quenching of MPA-capped CdS QDs, where binding of Ni(II) occurs with carboxylate group of mercapto acid as discussed in our previous report [2]. The spectra of the Cd 3d, S 2p and Ni 2p levels are shown in Fig. 8A, B and C, respectively. The appearance of Cd $3d_{5/2}$ peak at 405 eV, Cd $3d_{3/2}$ peak at 411.8 eV and S $2p_{3/2}$ peak at 161.8 eV confirm the presence of cadmium and sulfur in the CdS QDs [12,63]. After addition of nickel ion (50 μM) to MPA-CdS QDs, no peak, corresponding to Ni $2p_{3/2}$ at ~855.9 eV and Ni $2p_{1/2}$ at ~873.6 eV [64] appears which indicates that the binding of Ni doesn't occur onto the nanocrystal surface.

3.6. Possible role of the pendent methyl group of TLA on metal sensing selectivity

Generally, in mercapto acids capped QDs, the sulfur atom of the thiol group remains attached to the particle surface and the negatively charged carboxyl group (at high pH) remains exposed toward the solvent. In aqueous solution electrostatic repulsion between the negatively charged carboxylate groups of different particle units provides colloidal stability. When metal ions are added to the aqueous solution of mercapto acids capped QDs, they can be adsorbed onto the QD surface through interaction with soft sulfur centre or can coordinate with hard oxygen centre of water-exposed carboxylate group. In either of these two processes metal can affect the PL of QDs, i.e., enhancement or quenching of PL can occur. Now, interaction of metals with these two sites can depend on the structure of mercapto acids (capping ligands). In case of straight chain mercapto acids, such as TGA and MPA, metals can equally interact with both the sites. One can achieve the site selective interaction either by increasing surface coating [31] or by decreasing pH of the medium [65]. Increase of surface coating prevents the approach of metals to the QD surface. Xia et al. reported [31] that Cu(II) and Ag(I) can quench the PL of TGA-capped CdTe QDs through adsorption onto the particle surface; whereas electron transfer between Hg(II) and capping ligands is responsible for the PL quenching effect of Hg(II). In order to block the access of particle surface toward metals, the original TGA-capped CdTe QDs were further coated by denatured bovine serum albumin (dBSA). In this way, they have observed the site selective quenching of dBSA-coated CdTe QDs only by Hg(II) because the dBSA shell-layer effectively prevents the approach of Cu(II) and Ag(I) toward the QD surface. On the other hand, decrease in pH of the medium prevents the binding of metals with carboxylate group of mercapto acids due to the protonation at low pH. But acidic pH will destabilize the colloidal solution of QDs, possibly due to decrease in electrostatic repulsion between the particles through protonation of carboxylate group of mercapto acids. Gore et al. proposed the selective detection of Co(II) by TGA-capped CdS QDs through binding with carboxylate group of mercapto acid [65]. In a pH variation study, they have observed that the most sensitive pH lies within the range from 6.0 to 9.0 in order to get full complexation.

Use of TLA, a branched mercapto acid, as a capping ligand, directs the metal toward the exclusive surface adsorption by QDs even at basic pH (at high colloidal stability of QD solution). The environment around the QDs becomes crowded by the attachment of lots of capping ligands on the small QD surface. The crowding becomes more with side chain alkyl-group-containing mercapto acids capping ligands, such as TLA in lieu of MPA. When metal tends to bind the carboxylate group of mercapto acid (as represented in Fig. 9), the pendant methyl group in the side chain of TLA brings in somewhat unfavorably crowded environment and this reduces binding. The so called steric hindrance of methyl side chain (as observed by Fang et al. in case of 3-mercaptobutyric acid [28]) is responsible for the inhibition of binding of metals with carboxylate group of mercapto acid. Therefore, surface adsorption of Ag(I) takes place exclusively on our synthesized TLA-capped CdTe QDs which results in PL quenching. Selective turn-off PL-based sensing of Ag(I) by TLA-capped ZnS QDs at pH 7.5 [32] also supports the exclusive surface adsorption of QDs by metal in presence of TLA as capping ligand.

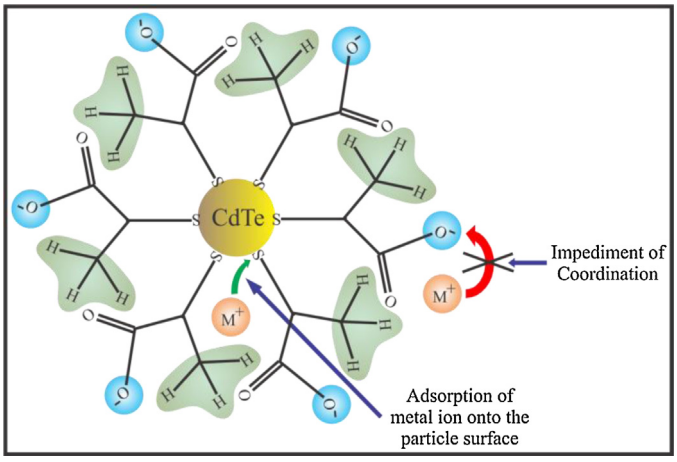

Fig. 9. Schematic representation of the sensing selectivity of TLA-capped CdTe QDs toward metal ion detection.

4. Conclusion

In conclusion, the effect of the pendant methyl group in the side chain of TLA on the synthesis and sensing selectivity of TLA-CdTe QDs has been demonstrated. The side chain methyl group of TLA confines the carboxyl group and suppresses the aggregation of QDs by preventing secondary coordination between the carboxyl oxygen of mercapto acid on the surface of CdTe nanocrystals with cadmium on the surface of the other. This facilitates the emergence of highly luminescent QDs with appropriate surface passivation.

The side chain methyl group of TLA also facilitates the selective interaction of metal ions onto the QDs surface even at basic pH, when carboxyl group of mercapto acid remains deprotonated. Thus, selective adsorption of Ag(I) onto the TLA-CdTe QD surface, results in PL quenching of QDs *via* stimulation of the nonradiative electron/hole recombination. The LOD of Ag(I) is found to be 50 nM. The present method provides a simple, rapid and ultrasensitive PL-based assay for the selective detection of Ag(I) without any interference of other commonly coexisting metal ions and also in real environmental water samples. Herein, for the first time, we attempted to demonstrate the importance of the structural effect of TLA as capping agent toward metal sensing selectivity of QDs and the possible origin of metal-sensing exclusiveness. This study puts forward a novel approach on the selection of capping ligands toward controlling of the metal sensing property of QDs. These results can be very useful toward the development of sensors by selecting and designing the appropriate capping ligands for the QDs.

Competing interest

The authors declare no competing financial interest.

Acknowledgements

MH thanks DST SERB-India (Fund no. SB/S1/PC-041/2013) for financial support. SP thanks UGC-India for the individual

fellowship. Sincere thanks are also due to Prof. S. Basu, Head, Chemical Sciences Division, Saha Institute of Nuclear Physics, Kolkata for allowing us to measure time-resolved photoluminescence decay in her departmental TCSPC setup. We are also thankful to Department of Physics, IIT Kharagpur, for allowing us to measure XPS data in their DST-FIST supported facility. We thank the anonymous reviewer for critical comments.

Appendix A. Supplementary data

Supplementary data associated with this article can be found, in the online version, at http://dx.doi.org/10.1016/j.snb.2016.08.127.

References

[1] D.A. Wheeler, J.Z. Zhang, Exciton dynamics in semiconductor nanocrystals, Adv. Mater. 25 (2013) 2878–2896.
[2] N. Mahapatra, S. Panja, A. Mandal, M. Halder, A single source-precursor route for the one-pot synthesis of highly luminescent CdS quantum dots as ultra-sensitive and selective photoluminescence sensor for Co^{2+} and Ni^{2+} ions, J. Mater. Chem. C 2 (2014) 7373–7384.
[3] G. Sagarzazu, Y. Kobayashi, N. Murase, P. Yang, N. Tamai, Auger recombination dynamics in hybrid silica-coated CdTe nanocrystals, Phys. Chem. Chem. Phys. 13 (2011) 3227–3230.
[4] S.J. Zhuo, J.J. Gong, P. Zhang, C.Q. Zhu, High-throughput and rapid fluorescent visualization sensor of urinary citrate by CdTe quantum dots, Talanta 141 (2015) 21–25.
[5] S.V. Kershaw, A.S. Susha, A.L. Rogach, Narrow bandgap colloidal metal chalcogenide quantum dots: synthetic methods, heterostructures, assemblies, electronic and infrared optical properties, Chem. Soc. Rev. 42 (2013) 3033–3087.
[6] T.Y. Zhai, X.S. Fang, L. Li, Y. Bando, D. Golberg, One-dimensional CdS nanostructures: synthesis, properties, and applications, Nanoscale 2 (2010) 168–187.
[7] X.Q. Fu, J.Y. Liu, Y.T. Wan, X.M. Zhang, F.L. Meng, J.H. Liu, Preparation of a leaf-like CdS micro-/nanostructure and its enhanced gas-sensing properties for detecting volatile organic compounds, J. Mater. Chem. 22 (2012) 17782–17791.
[8] R. Freeman, I. Willner, Optical molecular sensing with semiconductor quantum dots (QDs), Chem. Soc. Rev. 41 (2012) 4067–4085.
[9] X.D. Wang, O.S. Wolfbeis, R.J. Meier, Luminescent probes and sensors for temperature, Chem. Soc. Rev. 42 (2013) 7834–7869.
[10] V. Rajendran, M. Lehnig, C.M. Niemeyer, Photocatalytic activity of colloidal CdS nanoparticles with different capping ligands, J. Mater. Chem. 19 (2009) 6348–6353.
[11] R.S. Selinsky, Q. Ding, M.S. Faber, J.C. Wright, S. Jin, Quantum dot nanoscale heterostructures for solar energy conversion, Chem. Soc. Rev. 42 (2013) 2963–2985.
[12] M. Shen, W.P. Jia, Y.J. You, Y. Hu, F. Li, S.D. Tian, J. Li, Y.X. Jin, D.M. Han, Luminescent properties of CdTe quantum dots synthesized using 3-mercaptopropionic acid reduction of tellurium dioxide directly, Nanoscale Res. Lett. 8 (2013) 253.
[13] Q. Maa, X. Su, Recent advances and applications in QDs-based sensors, Analyst 136 (2011) 4883–4893.
[14] J. Nicolas, S. Mura, D. Brambilla, N. Mackiewicza, P. Couvreur, Design, functionalization strategies and biomedical applications of targeted biodegradable/biocompatible polymer-based nanocarriers for drug delivery, Chem. Soc. Rev. 42 (2013) 1147–1235.
[15] T.L. Doanea, C. Burda, The unique role of nanoparticles in nanomedicine: imaging, drug delivery and therapy, Chem. Soc. Rev. 41 (2012) 2885–2911.
[16] R.P. Singh, E.R. Pambid, Selective separation of silver from waste solutions on Chromium(III) Hexacyanoferrate(III) ion-Exchanger, Analyst 115 (1990) 301–304.
[17] M. Montalti, A. Cantellia, G. Battistelli, Nanodiamonds and silicon quantum dots: ultrastable and biocompatible luminescent nanoprobes for long-term bioimaging, Chem. Soc. Rev. 44 (2015) 4853–4921.
[18] G.L. Wang, Y.M. Dong, H.X. Yang, Z.J. Li, Ultrasensitive cysteine sensing using citrate-capped CdS quantum dots, Talanta 83 (2011) 943–947.
[19] W. Yin, H. Liu, M.Z. Yates, H. Du, F. Jiang, L. Guo, T.D. Krauss, Fluorescent quantum dot-polymer nanocomposite particles by Emulsiflcation/Solvent evaporation, Chem. Mater. 19 (2007) 2930–2936.
[20] B. Cormary, F. Dumestre, N. Liakakos, K. Soulantica, B. Chaudret, Organometallic precursors of nano-objects, a critical view, Dalton Trans. 42 (2013) 12546–12553.
[21] J. Chang, E.R. Waclawik, Colloidal semiconductor nanocrystals: controlled synthesis and surface chemistry in organic media, RSC Adv. 4 (2014) 23505–23527.
[22] V. Lesnyak, N. Gaponik, A. Eychmuller, Colloidal semiconductor nanocrystals: the aqueous approach, Chem. Soc. Rev. 42 (2013) 2905–2929.
[23] S. Sapra, J. Nanda, D.D. Sarma, F.A. El-Al, G. Hodes, Blue emission from cysteine ester passivated cadmium sulfide nanoclusters, Chem. Commun. 37 (2001) 2188–2189.
[24] H. Mattoussi, J.M. Mauro, E.R. Goldman, G.P. Anderson, V.C. Sundar, F.V. Mikulec, M.G. Bawendi, Self-assembly of CdSe-ZnS quantum dot bioconjugates using an engineered recombinant protein, J. Am. Chem. Soc. 122 (2000) 12142–12150.
[25] S.J. Lim, B. Chon, T. Joo, S.K. Shin, Synthesis and characterization of zinc-blende CdSe-based core/shell nanocrystals and their luminescence in water, J. Phys. Chem. C 112 (2008) 1744–1747.
[26] Y.L. Li, L.H. Jing, R.R. Qiao, M.Y. Gao, Aqueous synthesis of CdTe nanocrystals: progresses and perspectives, Chem. Commun. 47 (2011) 9293–9311.
[27] N. Gaponik, A.L. Rogach, Thiol-capped CdTe nanocrystals: progress and perspectives of the related research fields, Phys. Chem. Chem. Phys. 12 (2010) 8685–8693.
[28] T. Fang, K.G. Ma, L.L. Ma, J.Y. Bai, X. Li, H.H. Song, H.Q. Guo, 3-Mercaptobutyric acid as an effective capping agent for highly luminescent CdTe quantum dots: new insight into the selection of mercapto acids, J. Phys. Chem. C 116 (2012) 12346–12352.
[29] H. Zhang, D.Y. Wang, H. Mohwald, Ligand-selective aqueous synthesis of one-dimensional CdTe nanostructures, Angew. Chem. Int. Ed. 45 (2006) 748–751.
[30] H.Y. Acar, R. Kas, E. Yurtsever, C. Ozen, I. Lieberwirth, Emergence of 2 MPA as an effective coating for highly stable and luminescent quantum dots, J. Phys. Chem. C 113 (2009) 10005–10012.
[31] Y.S. Xia, C.Q. Zhu, Use of surface-modified CdTe quantum dots as fluorescent probes in sensing mercury (II), Talanta 75 (2008) 215–221.
[32] A. Mandal, A. Dandapat, G. De, Magic sized ZnS quantum dots as a highly sensitive and selective fluorescence sensor probe for Ag^+ ions, Analyst 137 (2012) 765–772.
[33] C.L. Huang, C.C. Huang, F.D. Mai, C.L. Yen, S.H. Tzing, H.T. Hsieh, Y.C. Lingd, J.Y. Chang, Application of paramagnetic graphene quantum dots as a platform for simultaneous dual-modality bioimaging and tumor-targeted drug delivery, J. Mater. Chem. B 3 (2015) 651–664.
[34] C. Wang, W. Zhai, Y. Wang, P. Yua, L. Mao, MnO_2 nanosheets based fluorescent sensing platform with organic dyes as a probe with excellent analytical properties, Analyst 140 (2015) 4021–4029.
[35] G.Q. Chen, Z. Guo, G.M. Zeng, L. Tang, Fluorescent and colorimetric sensors for environmental mercury detection, Analyst 140 (2015) 5400–5443.
[36] Y.S. Xia, C. Cao, C.Q. Zhu, Two distinct photoluminescence responses of CdTe quantum dots to Ag (I), J. Lumin. 128 (2008) 166–172.
[37] C. Marambio-Jones, E.M.V. Hoek, A review of the antibacterial effects of silver nanomaterials and potential implications for human health and the environment, J. Nanoparticle Res. 12 (2010) 1531–1551.
[38] P.L. Drake, K.J. Hazelwood, Exposure-related health effects of silver and silver compounds: a review, Ann. Occup. Hyg. 49 (2005) 575–585.
[39] J.F. Zhang, Y. Zhou, J. Yoon, J.S. Kim, Recent progress in fluorescent and colorimetric chemosensors for detection of precious metal ions (silver, gold and platinum ions), Chem. Soc. Rev. 40 (2011) 3416–3429.
[40] M.A. Butkus, M.P. Labare, J.A. Starke, K. Moon, M. Talbot, Use of aqueous silver to enhance inactivation of coliphage MS-2 by UV disinfection, Appl. Environ. Microbiol. 70 (2004) 2848–2853.
[41] N.R. Bury, F. Galvez, C.M. Wood, Effects of chloride, calcium, and dissolved organic carbon on silver toxicity: comparison between rainbow trout and fathead minnows, Environ. Toxicol. Chem. 18 (1999) 56–62.
[42] Q.L. Feng, J. Wu, G.Q. Chen, F.Z. Cui, T.N. Kim, J.O. Kim, A mechanistic study of the antibacterial effect of silver ions on Escherichia coli and Staphylococcus aureus, J. Biomed. Mater. Res. 52 (2000) 662–668.
[43] B.H. Zhang, L. Qi, F.Y. Wu, Functionalized manganese-doped zinc sulfide core/shell quantum dots as selective fluorescent chemodosimeters for silver ion, Microchim. Acta 170 (2010) 147–153.
[44] T.T. Gan, Y.J. Zhang, N.J. Zhao, X. Xiao, G.F. Yin, S.H. Yu, H.B. Wang, J.B. Duan, C.Y. Shi, W.Q. Liu, Hydrothermal synthetic mercaptopropionic acid stabled CdTe quantum dots as fluorescent probes for detection of Ag^+, Spectrochim. Acta Mol. Biomol. Spectrosc. 99 (2012) 62–68.
[45] H. Zhang, Z. Zhou, B. Yang, M.Y. Gao, The influence of carboxyl groups on the photoluminescence of mercaptocarboxylic acid-stabilized CdTe nanoparticles, J. Phys. Chem. B 107 (2003) 8–13.
[46] Z.H. Yu, J.B. Li, D.B. O'Connor, L.W. Wang, P.F. Barbara, Large resonant stokes shift in CdS nanocrystals, J. Phys. Chem. B 107 (2003) 5670–5674.
[47] A.L. Rogach, T. Franzl, T.A. Klar, J. Feldmann, N. Gaponik, V. Lesnyak, A. Shavel, A. Eychmuller, Y.P. Rakovich, J.F. Donegan, Aqueous synthesis of thiol-capped CdTe nanocrystals: state-of-the-art, J. Phys. Chem. C 111 (2007) 14628–14637.
[48] A. Mandal, N. Tamai, Influence of acid on luminescence properties of thioglycolic acid-capped CdTe quantum dots, J. Phys. Chem. C 112 (2008) 8244–8250.
[49] V.I. Klimov, D.W. McBranch, C.A. Leatherdale, M.G. Bawendi, Electron and hole relaxation pathways in semiconductor quantum dots, Phys. Rev. B 60 (1999) 13740–13749.
[50] S.F. Wuister, C.D. Donega, A. Meijerink, Influence of thiol capping on the exciton luminescence and decay kinetics of CdTe and CdSe quantum, J. Phys. Chem. B 108 (2004) 17393–17397.
[51] N. Mahapatra, S. Datta, M. Halder, A new spectroscopic protocol for selective detection of water soluble sulfides and cyanides: use of Ag-nanoparticles synthesized by Ag(I)-reduction via photo-degradation of azo-food-colorants, J. Photochem. Photobiol. A 275 (2014) 72–80.

[52] J.H. Jonte, D.S. Martin, The solubility of silver chloride and the formation of complexes in chloride solution, J. Am. Chem. Soc. 74 (1952) 2052–2054.
[53] R. Ramette, Solubility and equilibria of silver chloride, J. Chem. Educ. 37 (1960) 348–354.
[54] A.V. Isarov, J. Chrysochoos, Optical and photochemical properties of nonstoichiometric cadmium sulfide nanoparticles: surface modification with copper(II) ions, Langmuir 13 (1997) 3142–3149.
[55] S.F. Wuister, I. Swart, F. van Driel, S.G. Hickey, C.D. Donega, Highly luminescent water-soluble CdTe quantum dots, Nano Lett. 3 (2003) 503–507.
[56] C.W. Wang, M.G. Moffitt, Surface-tunable photoluminescence from block copolymer-stabilized cadmium sulfide quantum dots, Langmuir 20 (2004) 11784–11796.
[57] D. Hayes, O.I. Micic, M.T. Nenadovic, V. Swayambunathan, D. Meisel, Radiolytic production and properties of ultrasmall cds particles, J. Phys. Chem. 93 (1989) 4603–4608.
[58] A.S. Susha, A.M. Javier, W.J. Parak, A.L. Rogach, Luminescent CdTe nanocrystals as ion probes and pH sensors in aqueous solutions, Colloids Surf. A 281 (2006) 40–43.
[59] R. van Beek, A.P. Zoombelt, L.W. Jenneskens, C.A. van Walree, C.D. Donega, D. Veldman, R.A.J. Janssen, Side chain mediated electronic contact between a tetrahydro-4 H-thiopyran-4-ylidene-appended polythiophene and CdTe quantum dots, Chem. Eur. J. 12 (2006) 8075–8083.
[60] Y.B. Lou, Y.X. Zhao, J.X. Chen, J.J. Zhu, Metal ions optical sensing by semiconductor quantum dots, J. Mater. Chem. C 2 (2014) 595–613.
[61] S. Akshya, P.S. Hariharan, V.V. Kumar, S.P. Anthony, Surface functionalized fluorescent CdS QDs: selective fluorescence switching and quenching by Cu^{2+} and Hg^{2+} at wide pH range, Spectrochim. Acta Mol. Biomol. Spectrosc. 135 (2015) 335–341.
[62] Y.G. Ko, S.W. Karng, G.S. Lee, U.S. Choi, Smart glass substrate as colorimetric chemosensor for highly selective detection of silver ion, Sens. Actuators B 177 (2013) 1107–1114.
[63] J.L. Gautier, J.P. Monras, I.O. Osorio-Roman, C.C. Vasquez, D. Bravo, T. Herranz, J.F. Marco, J.M. Perez-Donoso, Surface characterization of GSH-CdTe quantum dots, Mater. Chem. Phys. 140 (2013) 113–118.
[64] P. Prieto, V. Nistor, K. Nouneh, M. Oyama, M. Abd-Lefdil, R. Diaz, XPS study of silver, nickel and bimetallic silver-nickel nanoparticles prepared by seed-mediated growth, Appl. Surf. Sci. 258 (2012) 8807–8813.
[65] A.H. Gore, D.B. Gunjal, M.R. Kokate, V. Sudarsan, P.V. Anbhule, S.R. Patil, G.B. Kolekar, Highly selective and sensitive recognition of Cobalt(II) ions directly in aqueous solution using carboxyl-Functionalized CdS quantum dots as a naked eye colorimetric probe: applications to environmental analysis, ACS Appl. Mater. Interfaces 4 (2012) 5217–5226.

Biographies

Dr. Niharendu Mahapatra, Ph. D: M.Sc. (Physical Chemistry), Ph.D. in Chemistry. Currently, Postdoc at the Department of Electrical Engineering – Physical Electronics, School of Electrical Engineering, Tel Aviv University, Ramat Aviv, Israel.

Dr. Abhijit Mandal, Ph. D. Currently, Assistant Professor, Department of Chemistry and Environment, Heritage Institute of Technology, Kolkata-700107.

Sudipta Panja, M. Sc. (Physical Chemistry). Currently, Graduate Student, IIT Kharagpur Chemistry, India.

Prof. Mintu Halder, Ph. D., Associate Professor in Chemistry, Indian Institute of Technology, Kharagpur, India.